Langmuir
Article
pubs.acs.org/Langmuir

Synthesis of Size-Monodisperse Spherical Ag@SiO$_2$ Nanoparticles and 3-D Assembly Assisted by Microfluidics

P. Massé, S. Mornet, E. Duguet, and M. Tréguer-Delapierre*

CNRS, University of Bordeaux, ICMCB, UPR 9048, F-33600 Pessac, France

S. Ravaine

CNRS, University of Bordeaux, CRPP, UPR 8641, F-33600 Pessac, France

A. Iazzolino, J.B. Salmon, and J. Leng

CNRS, University of Bordeaux, RHODIA, LOF, UMR 5258, F-33600 Pessac, France

Supporting Information

ABSTRACT: This article reports a one-step approach for the fabrication of highly uniform, spherical Ag particles with tailored dimensions ranging from 10 to 30 nm. Coated with silica shell, the high uniformity of the particles allows their spontaneous assembly into millimeter-long extended 3-D arrays with transverse dimensions of tens of micrometers, using a microfluidic evaporation-based process.

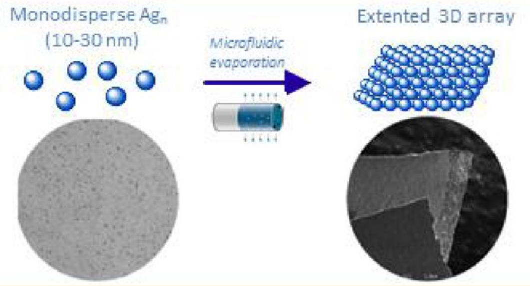

INTRODUCTION

The synthesis of uniform nano-objects in large quantities as building blocks for manufacturing materials with new properties or functions is one of the major challenges in nanotechnology. Among them, silver nanoparticles have received considerable interest because of their fascinating chemical and physical properties.[1−5] Geometrical arrangements integrating several Ag nanostructures with feature sizes smaller than the wavelength of light display promising properties and may lead to a variety of innovative applications, e.g., active components to focus, guide, and manipulate light.[6−10] This makes the controlled assembly of simple Ag nanostructures into extended networks a topic of intense research in materials science.[6,10,11] Methods based on colloidal assembly are among the most promising bottom-up approaches.[12−16] All these methods typically require monodisperse particles coated with an appropriate stabilizer and dispersed in a suitable solvent. Despite the myriad of synthetic protocols reported over the past 30 years for the preparation of Ag particles with any desired geometry,[17−25] notably lacking is a simple and robust procedure for the preparation of a large number of spheroidal particles with diameter larger over 15 nm with relatively narrow distribution in size.

In this article, we present a one-step approach for the fabrication of homogeneous silver spheres with dimensions ranging in diameter from 10 to 30 nm with small size variance. The method is a simple modification of the conventional polyol approach,[19,21,22] where sulfide ions were used to avoid the formation of cubic or other anisotropic shapes. This is based on previous findings from silver photographic technology where the presence of traces of sulfides and polysulfides, in the range of ppm, affects particle growth by accelerating the rate of silver ion reduction.[27,28] In our case, an aged sulfide ion solution was introduced in the reaction medium. Due to the low solubility of silver sulfide species, $(Ag_2S)_n$ nanocrystallites form immediately and serve as a catalyst for the reduction of silver ion. Thereby, the introduction of sulfide ions results in the fabrication of spherical particles bounded by lower-energy surface facets. The as-obtained Ag particles have been proven to be compatible with the Stöber process and thus can be easily coated with silica of arbitrary thickness without any purification while preserving their monodispersity. The high monodispersity of the prepared Ag@SiO$_2$ spheres renders them perfectly suitable for colloidal array formation using an original microfluidic approach based on evaporation.[29−31] Compared to all the self- or guided-assembly techniques based on evaporation, this confined drying experiment permits a better control of the evaporation flux and transport phenomena, prevents phenomena such as capillary effects, and leads to an easy way to assemble nanoparticles into dense arrays starting from dilute stock solutions. It also permits control of the shape-up process of the material in a geometry

Received: October 3, 2012
Revised: January 10, 2013
Published: January 10, 2013

dx.doi.org/10.1021/la3039335 | *Langmuir* 2013, 29, 1790−1795

that is defined by that of the microchannels and leads to 3D samples with neat surfaces adequate for optical characterization.

■ EXPERIMENTAL SECTION

Materials. Sodium hydrosulfide (NaHS), poly(vinylpyrrolidone) (PVP; $M_w \approx 55\,000$), silver nitrate ($AgNO_3$; 99.998%), and tetraethyl orthosilicate (TEOS) were purchased from Sigma-Aldrich. Ethylene glycol (EG, cat. No.9300) and ammonia solution (27−30 wt %) were obtained from J.T. Baker. Absolute ethanol was purchased from Scharlau. All reagents and solvents were used without further purification.

Synthesis of Ag Spherical Nanoparticles. First, a 30 mM solution of NaHS in EG was prepared and aged for a controlled time. As explained in the following section, the aging time is a critical parameter in this study. A 60-mL sample of EG was then heated and stirred in a 250-mL flask at 150 °C for 2 h. The reactor was degassed with Argon during the reaction. After 30 min, 35 μL of the aged NaHS solution and 15 mL of a PVP solution in EG (30 mg/mL) were injected in the reaction medium. A 5-mL sample of a 0.16 M $AgNO_3$ solution in EG was then prepared and added to the reaction medium. The solution turned yellow immediately. The reaction was quenched by quickly cooling the reaction flask in an ice-cold water bath. This halts the growth and prevents the particles from fast aggregation and ripening. The Ag nanoparticles were then washed with ethanol by centrifugation redispersion cycles ($\sim$3) and finally redispersed in absolute ethanol to a final silver concentration of 1.6 g/L.

Encapsulation in Silica. The resulting silver nanoparticles were then coated with silica by using a modification of a previously reported method.[32,33] Typically, 3.75 mL of the Ag nanoparticles dispersion was mixed under continuous magnetic stirring with a solution of deionized water and ammonia, at a volume ratio of 93.8/5/1.2 for absolute ethanol, water, and ammonia, respectively. By varying the amount of silica precursor, core−shell with a wide range of silica shell thickness could be synthesized. For example, for silica thickness of 5, 22, and 18 nm (Ag_n diameter = 22 nm), 10, 22, or 70 μL of tetraorthosilicate were added, respectively, and the reaction mixtures were stirred for 12 h at $\sim$20 °C. Upon completion of the growth of silica shell, the particles were washed with ethanol and water and redispersed in water.

Microfluidics-Assisted Assembly. The Ag@SiO_2 particles were self-assembled into a 3D extended array by introducing a few microliters of their aqueous suspension (typical concentration $\approx 10^{17}$ particles/L) onto a microfluidic evaporator device. The permeation-based microfluidic device was made of a polydimethylsiloxane (PDMS) membrane permeable to molecular liquids and gases, but not to nanoparticles. A schematic representation of the evaporator is shown in Figure 1. More details could be found elsewhere.[29−31] The device was made of a capillary, one wall made of a PDMS membrane (Figure 1, top) across which solvent may permeate; it was connected to a large (microliter) reservoir. Upon the extraction process, lost solvent (water) was replenished by a spontaneous flux coming from the reservoir, which in turn brings more and more particles from the dispersion in the reservoir. Consequently, the nanoparticles get trapped at the tip of the capillary while being steadily concentrated by the permeation-induced flux. Once the nanoparticles reached a given concentration, densification of the particles took place leading to a dense state of nanoparticles growing from the tip of the capillary. The conditions required for a successful guided-assembly stem from the colloidal stability of the particles to assemble. Here, we focus on silica-coated nanoparticles where the silica provides the electrosteric repulsion necessary to the stability. It would be possible to achieve the same type of assembly for the silver nanoparticles if their natural charge is sufficient to grant the colloidal stability at high concentration. A steric protection with amino- or thiol-terminated PEG for instance would lead to very stable arrays.

Characterization. Transmission electron microscopy (TEM) was carried out with a Philips CM20 microscope operating at 75 kV. Samples were prepared on a carbon-coated copper grid by evaporating a drop of the nanoparticle colloidal dispersions. TEM images were used for the statistical computation of average size and the standard distribution on the minimal basis of 1000 particles per batch. High-resolution transmission electron microscopy (HRTEM) analyses were performed by using a JEOL 2000FX microscope. SEM images were collected on a JSM 6700F after extraction of the dense arrays of nanoparticles out of the permeation-based microfluidic device. The extraction was performed by peeling off the PDMS membrane; the resulting material was collected by stamping it onto carbon tape. Absorption spectra of the silver nanoparticles dispersions were collected with a UV-3600 Shimadzu UV−vis−NIR spectrophotometer using quartz cells with a 10-mm optical path length. Extinction spectra of the manufactured dense arrays of Ag@SiO_2 nanoparticles were recorded by using an optical-fiber based spectrometer (Avantes, AvaSpec-3648) attached to a microscope (Olympus, IX71), and using an halogen lamp that irradiates the sample (without any condenser). Transmitted light through the whole system (PDMS microfluidic chip and the dense array confined in the microchannel, height 5 μm) was collected with a 20× magnification objective (Olympus, NA 0.45). Reference spectra were collected from the transmission of light through the PDMS slab only. Due to the finite numerical aperture of our device, we could not assume that the spectrometer did not collect some scattered light at low angles. The spatial resolution of the measurements was around 4 μm × 4 μm.

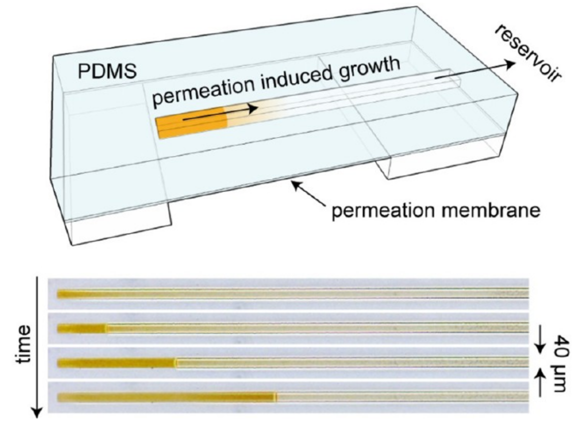

Figure 1. Top: Sketch of the evaporation-based microfluidic device where a channel is in contact with a membrane that permits the extract of the solvent only, not the solute (thickness of the channel $\sim$10 μm, width $\sim$40 μm, evaporation length 1 cm, thickness of the membrane $\sim$10 μm). This latter gets more and more concentrated until a dense state grows (typical growth rate $\sim$10 μm/s). Bottom: Optical snapshots showing the progressive formation of a dense state of Ag@SiO_2 particles (time lapse between pictures $\sim$6 min). After a transient period during which yellow tint appears (and witness the concentration process), self-assembly leads to millimeter long linear colloidal lattices with a packing volume fraction of about 60%.

■ RESULTS AND DISCUSSION

Monodisperse spherical silver particles with average diameters up to 30 nm were prepared by a synthetic polyol approach similar to those previously reported for the production of silver nanocubes.[33] However, the production of nanocubes was inhibited through addition of an aged solution of sulfide ions to the reaction medium. This method yielded highly monodisperse spherical particles up to 30 nm (Figures 2 and 3). The obtained particles were remarkably homogeneous. No trace of distinct populations of silver particles was found on the grids. TEM showed that, for all samples smaller than 30 nm, polydispersity never exceeded 7%. HRTEM studies on Ag nanopsheres were single crystal without twin defect in the lattice (Figure S1, Supporting Information). Above 30 nm, a noticeable deterioration of the monodispersity due to an

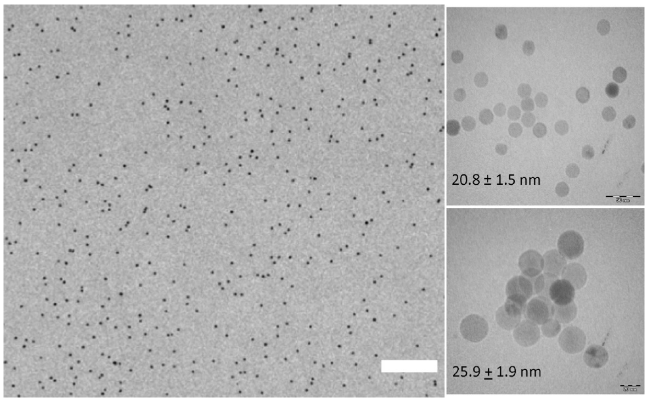

Figure 2. TEM micrographs of Ag particles of different sizes synthesized in the presence of 4 h-aged NaHS catalyst: (left) 15.3 nm; (right) 20.8 and 25.9 nm (scale bar of the main micrograph = 500 nm).

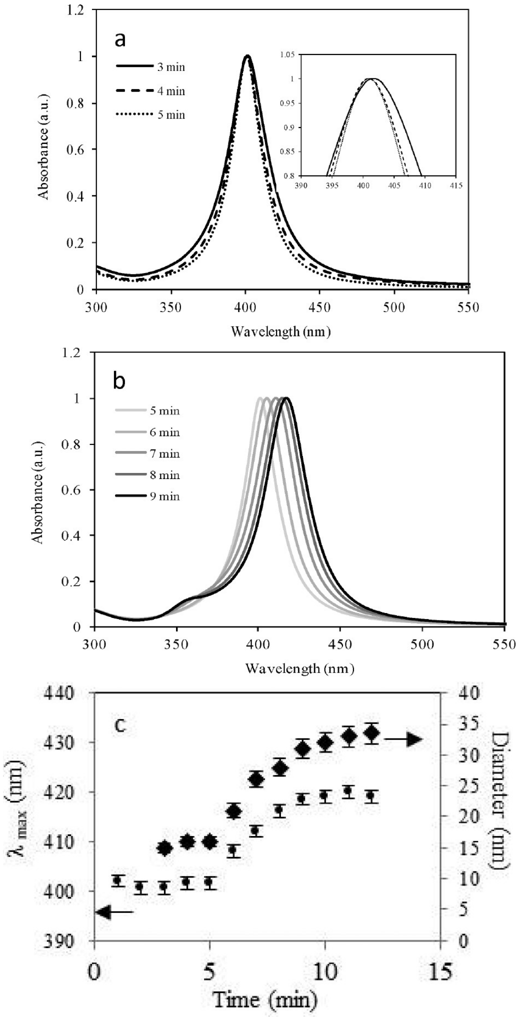

Figure 3. (a, b) Evolution of the extinction spectra of silver nanoparticles suspension with reaction time. Spectra were normalized at λ_{max} in order to facilitate the comparison. (c) Dependence of the diameter as well as the position of the spectral position of the dipole component of the plasmon resonance on the reaction time. Particle sizes were obtained by statistical analysis of the TEMs (Experimental Section).

increasing number of faceted particles was observed; it goes up to 15%. Optical properties of the obtained colloidal suspension were characterized by means of UV–vis spectroscopy (Figure 3). Silver particles display a very symmetrical plasmon band due to the small sizes. The plasmon band is characteristic of their dipolar plasmon mode. The absorption bands were narrow and approximately Gaussian. After an initial slight blue shift of a few nm (inset of Figure 3a) between 5 and 10 nm particles, when the diameter is increased up to 30 nm, there was a noticeable red shift up to 420 nm and band broadening (Figure 3b,c). For small size, it is well-known that the wavelength resonance is independent of the size of the homogeneous particle. The slight blue shifts of the plasmon band position observed at the early stage of the synthesis may originated from specific surface-related effects (adsorption of unreacted Ag^+, PVP macromolecules, oxidized aldehydes, ...).[35,36] As the particle size increased, the band red shifted. The observed trend agrees with the expected changes of the optical behavior for increasing particle size (predicted by Mie theory).[10,36] The broadening of the dipole plasmon band stems mainly from radiative losses. The narrow distribution of size observed is thought to be a direct consequence of the efficiency of the nucleation step in the presence of the sulfide catalyst by considering the nanoparticle growth in the classical nucleation/diffusional growth model. When a sufficient amount of catalyst is present in the reaction medium, a large number of silver atoms are produced instantaneously and the nucleation occurs only within an extremely short period of time. The silver atoms formed initially self-condensate to form a fixed number of seeds during the first stage of the reation, from which particles continue to grow by diffusion-driven deposition of silver atoms. The fast growth kinetics promoted the formation of only one dominant spherical product and not nonuniform or faceted ones. We confirmed this hypothesis by using fresh catalyst for the formation of Ag particles. Figure S2 in the Supporting Information shows the TEM image and the optical spectra recorded from the Ag particles that were grown in the presence of fresh catalyst. The reaction clearly took place in less uniform conditions. Furthermore, a clear lack of repeatability and consistency was observed. By comparing thoroughly the results obtained from different runs, we found that the use of a fresh NaHS solution led to irreproducible results in terms of size and size polydispersity. This was assigned to the complicated sulfur chemistry. In fresh solutions, the activity of HS^- species is low, whereas, in contrast, in aged solution, their activity is extremely high due to the formation of polysulfides. Their presence greatly shorten the time scale for $AgNO_3$ reduction by hundreds of folds, allowing the thermodynamically less favorable, single crystal seeds to form through a heterogeneous nucleation process. They strongly catalyze both the reduction and growth processes, and hence the production of uniform particles in a reproducible way.

Achieving good control over the particle size distribution required an optimization of the preheating atmosphere of the solvent before introduction of the reactants. Figure 4 shows the influence of the time of the preheating step of the solvent in air, before the system was flushed with Ar and the reactants were introduced in the reacting medium, on the optical properties of the Ag colloidal solutions. When the reaction was performed in oxygen saturated with ethylene glycol, a broad peak in the neighborhood of 405 nm developed (Figure 4, dotted line). When Ar-saturated ethylene glycol was tested, however, such a peak was not observed. The silver precursor reduction did

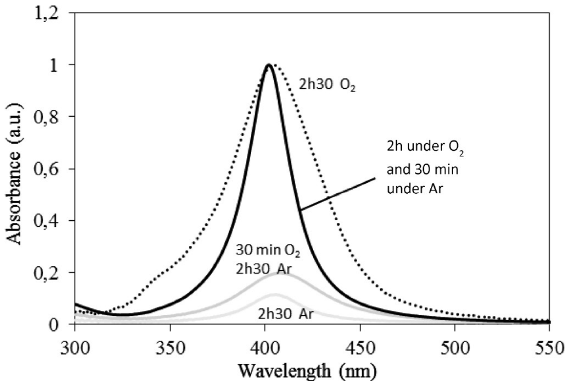

Figure 4. UV−visible spectra showing the importance of the time of the preheating step of ethylene glycol in air before flushing the solution with Ar on the formation of Ag nanoparticles: heating temperature 150 °C ; aging time of catalyst 4 h; reaction time 5 min.

occur, but at a much slower rate. Only a band with low intensity developed at 405 nm. As soon as the solvent was exposed to oxygen in the preheating period the plasmon resonance centered around 405 nm increased in intensity and became narrower with increasing the time of exposure. These observations suggest that an increase of the ratios of various aldehydes and ketones issued from the oxidation of the polyol to silver allows rapid seed formation at the initial stage of the reaction leading to high particle concentration in the final suspension and relatively fast particle growth. This is in agreement with the observations of Xia and co-workers who established the importance of the presence of aldehydes issued from oxidation of ethylene glycol in the process of reduction of silver ions.[37]

Given the relatively high monodispersity achieved by this reduction process, the method positions itself as a convenient approach to produce several grams of Ag particles in a single laboratory-scale reactor. By simply quenching the reaction with ice-cooled water, it was possible to obtain silver nanoparticles in the 10−30 nm size regime (Figure 3c). Despite their high monodispersity, their assembly in a microfluidic evaporation device leads to highly packed structure with defects and irregularities (see the Supporting Information). They may originate from colloidal instability at high concentration and salt precipitations. To improve their colloidal stability for further 3D assembly, the particles were encapsulated by a silica layer. Their encapsulation by the glass shell was performed by the well-established Stöber method.[32] Figure S3 in the Supporting Information depicts TEM images of the particles as well as the spectral changes observed from the silica deposition. The monodispersity was preserved. A red shift in the position of the absorption maximum as the shell thickness increased was observed due to the increase in the local refractive index around the particles.[33] Once introduced in a microfluidic evaporation device (Figure 1), the prepared Ag nanospheres readily formed large close-packed colloidal arrays upon progressive evaporation of the solvent. As outlined earlier, this device permits the enrichment of the silver nanoparticle dispersion to obtain densely packed nanoparticles. Figure 1 (bottom) shows optical images of the microfluidic channels at different times after the introduction of the monodisperse Ag@SiO_2 within (22 nm (core)/20 nm (shell)). After a transient period during which the dispersion turned a yellow color providing evidence of the concentration process, self-assembly of the particles (typical growth rate ≈ 1 μm/s) progressively led to millimeter long linear dense colloidal lattices. The interplay between evaporation as a driving force for inducing the self-assembly and the surface patterning for guiding the assembly[38−41] leads to the formation of extended arrays. The dynamics of the concentration process is controlled by the geometry of the device, the thickness of the membrane, and the initial concentration of the dispersion.[29−31] Figure 5a shows images of the material once transferred onto the SEM substrate. The linear structures that resulted from the self-assembly process could be recognized, yet fractures evidence that the material was degraded during the transfer. A closer SEM view (Figure 5b) shows that the structure was indeed three-dimensional, finely replicating the shape of the microfluidic channel. An even closer view from the top surface of the dense structure (Figure 5c) highlights the high degree of nanoparticle packing with a surface roughness of the same order as that of the nanoparticle size. A further magnification of the top plane in back scattering (Figure 5d, top) mode evidenced the location of the silver cores while direct imaging (Figure 5d, bottom) strongly suggests that the silica shell underwent some faceting during the concentration process. The structural characterization of the lattice was investigated by calculating the pair correlation function (Figure S5, Supporting Information). The analysis demonstrates that the nanoparticles underwent some degree of compression during drying and shows that the lattice is amorphous rather than perfectly crystalline. This could be due to the concentration process that is rapid and may prevent crystallization or the size distribution that is slightly above the minimum requested of crystallization (less 15% polydispersity).

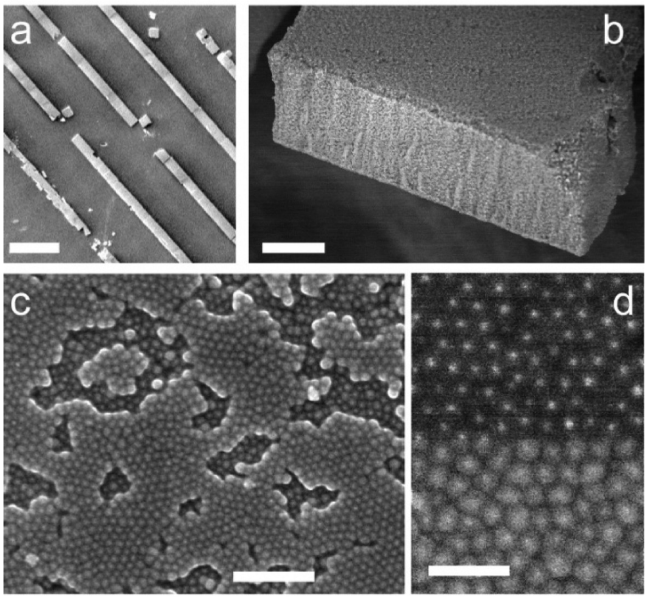

Figure 5. SEM characterization of the 3D nanoparticles assemblies after removal of the membrane. The dense material is stuck onto a SEM substrate and imaged at several degree of magnification. (a, b) Far view of the 3D Ag@SiO_2 nanoparticles networks: (a) scale bar = 100 μm; (b) scale bar = 10 μm. (c) Top view of the surface of the dense material, scale bar = 1 μm. (d) Composite SEM image in backscattering (top) and direct (bottom) imaging modes showing the silver cores, scale bar = 0.1 μm.

Typical spectra collected on-chip during the progressive assembly of the colloidal particles are shown in Figure 6. Far

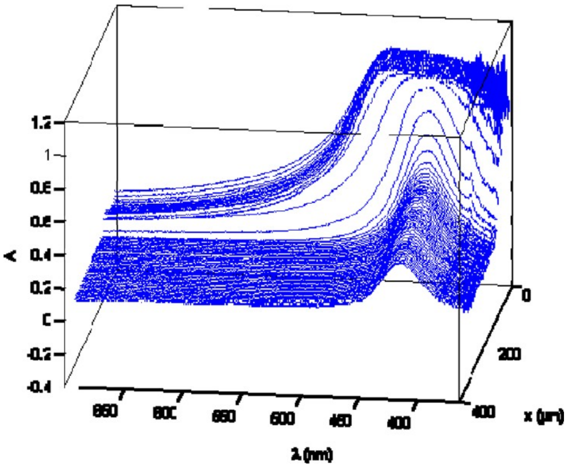

Figure 6. Evolution of the extinction spectra, measured on chip, during the self-assembly of the colloidal particles. (Front of the growing dense state (x = 400 μm); dense array of nanoparticles (x = 0 μm).)

from the growing dense state, extinction spectra matched absorption ones performed on the dilute dispersion in vials using conventional absorption spectrometry. Strong discrepancies were then observed upon progressive self-assembly of the nanoparticles within the microfluidic channel: a pronounced red shift and a broadening of the extinction are observable at lowest wavelengths. We are currently analyzing these fascinating optical features in detail, which probably could result from subtle effects such as plasmonic couplings or even a coupling with the photonic properties of the dense array. We also left for a future work the complete discussion of the spatiotemporal spectrometric measurements performed on-chip during the growth of the dense state.

CONCLUSION

We have demonstrated that by introducing an aged sulfide catalyst into the well-established polyol synthesis of silver nanoparticles, spherical nanocrystals with tunable sizes (10−30 nm) can be produced with high reproducibility. Their monodispersity and their surface compatibility with silica enables the facile formation of close-packed extended three-dimensional dense material using microfluidic setup based on evaporation. This latter provides a new tool for enriching opportunities for constructing nanostructure arrays not only of spherical particles but also of different geometrical parameters or multicomponents materials (metal-dielectric, quantum dots) with neat surfaces adequate for optical characterization. Compared to other self- or guided-assembly techniques based on evaporation, the present one takes full advantage of miniaturization. Due to high surface/volume ratio, evaporation is efficient and permits the concentration of stock solutions of resonant nanoparticles which are often dilute in a reasonable amount of time. The variety of future experiments which can be developed can reveal many interesting properties of such materials, which can be used for applications in many scientific as well as industrial areas such as optoelectronics, biotechnology, and plasmonic.

ASSOCIATED CONTENT

Supporting Information

Electron micrographs, spectra of nanoparticles, and details of 3D assembly of silver nanoparticles. This material is available free of charge via the Internet at http://pubs.acs.org.

AUTHOR INFORMATION

Corresponding Author

*E-mail: treguer@icmcb-bordeaux.cnrs.fr. Tel: +33 540 006 333. Fax: +33 540 002 761

Notes

The authors declare no competing financial interest.

ACKNOWLEDGMENTS

The European Community's Seventh Framework Programme (MetaChem project under grant agreement no. 228762) and the Conseil Régional d'Aquitaine are gratefully acknowledged for funding.

REFERENCES

(1) Cao, Y. C.; Jin, R.; Mirkin, C. A. Nanoparticles with Raman Spectroscopic Fingerprints for DNA and RNA Detection. *Science* **2002**, *297*, 1536−1540.

(2) Alivisatos, P. The Use of Nanocrystals in Biological Detection. *Nat. Biotechnol.* **2004**, *22*, 47−52.

(3) Pyayt, A. L.; Wiley, B.; Xia, Y.; Chen, A.; Dalton, L. Integration of Photonic and Silver Nanowire Plasmonic Waveguides. *Nat. Nanotechnol.* **2008**, *3*, 660−665.

(4) Banholzer, M. J.; Millstone, J. E.; Qin, L.; Mirkin, C. A. Rationally Designed Nanostructures for Surface-Enhanced Raman Spectroscopy. *Chem. Soc. Rev.* **2008**, *37*, 885−897.

(5) Krutyakov, Y. A.; Kudrinskiy, A. A.; Olenin, A. Y.; Lisichkin, G. V. Synthesis and Properties of Silver Nanoparticles: Advances and Prospects. *Russ. Chem. Rev.* **2008**, *77*, 233−257.

(6) Rycenga, M.; Cobley, C.; Zeng, J.; Li, W.; Moran, C.; Zhang, Q.; Qin, D.; Xia, Y. Controlling the Synthesis and Assembly of Silver Nanostructures for Plasmonic Applications. *Chem. Rev.* **2011**, *111*, 3669−3712.

(7) Romo-Herrera, J. M.; Avarez-Puebla, R. A.; Liz-Marzan, L. M. Controlled Assembly of Plasmonic Colloidal Nanoparticle Clusters. *Nanoscale* **2011**, *3*, 1304−1315.

(8) Simovski, C.; Tretyakov, S. Model of Isotropic Resonant Magnetism in the Visible Range based on Core-Shell Clusters. *Phys. Rev. B* **2009**, *79*, 045111.

(9) Girard, C.; Dujardin, E.; Baffou, G.; Quidant, R. Shaping and Manipulation of Light Fields with Bottom-Up Plasmonic Structures. *New J. Phys.* **2008**, *10*, 105016−105038.

(10) Fan, J. A.; Bao, K.; Wu, C.; Bao, J.; Bardhan, R.; Halas, N. J.; Manoharan, V. N.; Shvets, G.; Nordlander, P.; Capasso, F. Fano-like Interference in Self-Assembled Plasmonic Quadrumer Clusters. *Nano Lett.* **2010**, *10*, 4680−4685.

(11) Evanoff, D. D.; Chumanov, G. Synthesis and Optical Properties of Silver Nanoparticles and Arrays. *ChemPhysChem.* **2005**, *6*, 1221−1231.

(12) Zhang, Q.; Xie, J.; Yang, J.; Lee, J. Monodisperse Icosahedral Ag, Au and Pd Nanoparticles: Size Control Strategy and Superlattice Formation. *ACS Nano* **2009**, 3 (1), 139−148.

(13) Nie, Z. H.; Petukhova, A.; Kumacheva, E. Properties and Emerging Applications of Self-Assembled Structures Made from Inorganic Nanoparticles. *Nat. Nanotechnol.* **2010**, *5*, 15−25.

(14) Min, Y.; Akbulut, M.; Kristiansen, K.; Golan, Y.; Israelachvili, J. The Role of Interparticle and External Forces in Nanoparticle Assembly. *Nat. Mater.* **2008**, *7*, 527−538.

(15) Bishop, K. J. M.; Wilmer, C. E.; Soh, S.; Grzybowski, B. A. Nanoscale Forces and Their Uses in Self-Assembly. *Small* **2009**, *5*, 1600−1630.

(16) Zhang, J.; Li, Y.; Zhang, X.; Yang, B. Colloidal Self-Assembly Meets Nanofabrication: From Two-Dimensional Colloidal Crystals to Nanostructure Arrays. *Adv. Mater.* **2010**, *22*, 4249−4269.

(17) Xia, Y.; Xiong, Y.; Lim, B.; Skrabalak, S. Shape-Controlled Synthesis of Metal Nanocrystals: Simple Chemistry Meets Complex Physics? *Angew. Chem., Int. Ed.* **2009**, *48*, 60−103.

(18) Zhang, Q.; Xie, J.; Yu, Y.; Lee, J. Monodispersity Control in the Synthesis of Monometallic and Bimetallic Quasi-Spherical Gold and Silver Nanoparticles. *Nanoscale* **2010**, *2*, 1962−1975.

(19) Zhang, Q.; Cobley, C.; Au, L.; McKiernan, M.; Schwartz, A.; Wen, L.-P.; Chen, J.; Xia, Y. Production of Ag Nanocubes on a Scale of 0.1 g per Batch by Protecting the NaHS-Mediated Polyol Synthesis with Argon. *ACS Appl. Mater. Interfaces* **2009**, *1*, 2044−2048.

(20) Pyatenko A., M.; Yamaguchi, M.; Suzuki, M. Synthesis of Spherical Silver Nanoparticles with Controllable Sizes in Aqueous Solutions. *J. Phys. Chem. C* **2007**, *111*, 7910−7917.

(21) Silvert, P. Y.; Herrera-Urbina, R.; Duvauchelle, N.; Vijayakrishnan, V.; Tekaia-Elhissen, K. Preparation of Colloidal Silver Dispersions by the Polyol Process. Part 1. Synthesis and Characterization. *J. Mater. Chem.* **1996**, *6*, 573−577.

(22) Cobley, C. M.; Rycenga, M.; Zhou, Fei.; Li, Z.; Xia, Y. Controlled Etching as a Route to High Quality Silver Nanospheres for Optical Studies. *J. Phys. Chem. C* **2009**, *113*, 16975−16982.

(23) Dong, X.; Ji, X.; Wu, H.; Zhao, L.; Li, J.; Yang, W. Shape Control of Silver Nanoparticles by Stepwise Citrate Reduction. *J. Phys. Chem. C* **2009**, *113*, 6573−6576.

(24) Mafuné, F.; Kohno, J. Y.; Takeda, Y.; Kondow, T. Formation and Size Control of Silver Nanoparticles by Laser Ablation in Aqueous Solution. *J. Phys. Chem. B* **2000**, *104*, 9111−9117.

(25) Pastoriza-Santos, I.; Liz-Marzán, L. M. N,N-dimethylformamide as a reaction medium for metal nanoparticle synthesis. *Adv. Funct. Mater* **2009**, *19*, 679−688.

(26) Creighton, J. A.; Blatchford, C. G.; Albrecht, M. G. Plasma Resonance Enhnacement of Raman Scattering by Pryidine Adsorbed on Silver or Gold Sol Particles of Size Comparable to the Excitation Wavelength. *J. Chem. Soc., Faraday Trans. 2* **1979**, *75*, 790−798.

(27) Kryokov, A. I.; Zin'chuk, N. N.; Korzhak, A. V.; Kuchmii, S. Y. Catalysis of the reduction of silver ions by Ag_2S nanoparticles. *Theor. Exp. Chem.* **2001**, *37* (6), 355.

(28) Tani, T. In *The Theory of the Photographic Process*; Oxford University Press: New York, NY, 1995.

(29) Leng, J.; Lonetti, B.; Tabeling, P.; Joanicot, M.; Ajdari, A. Microevaporators for Kinetic Exploration of Phase Diagrams. *Phys. Rev. Lett.* **2006**, *96*, 084503.

(30) Salmon, J.-B.; Leng, J. Application of Microevaporators to Dynamic Exploration of the Phase Diagram. *J. Appl. Phys.* **2010**, *107*, 084905.

(31) Merlin, A.; Salmon, J.-B.; Leng, J. Microfluidic-Assisted Growth of Colloidal Crystals. *Soft Matter* **2012**, *8*, 3526−3537.

(32) Graf, C.; Vossen, D. L. J.; Imhof, A.; Van Blaaderen, A. A General Method to Coat Colloidal Particles With Silica. *Langmuir* **2003**, *19*, 6693−6700.

(33) Ung, T.; Liz-Marzan, L.; Mulvaney, P. Controlled Method for Silica-Coating of Silver Colloids. Influence of Coating on the Rate of Chemical Reactions. *Langmuir* **1998**, *14*, 3740−3748.

(34) Siekkinen, A.; Mc Lellan, M.; Chen, J.; Xia, Y. Rapid Synthesis of Small Silver Nanocubes by Mediating Polyol Reduction with a Trace Amount of Sodium Sulfide or Sodium Hydrosulfide. *Chem. Phys.Lett.* **2006**, *43*, 491−496.

(35) Henglein, A. Colloidal nanoparticles of semiconductor and metals: electronic structure and processes. *Ber. Bunsen-Ges.* **1990**, *94*, 600−603.

(36) Peng, S.; McMahon, J. M.; Schatz, G. C.; Gray, S. K.; Sun, Y. Reversing the size-dependence of surface plasmon resonances. *Proc. Natl. Acad. Sci. U.S.A.* **2010**, *107* (33), 14530−14534.

(37) Skrabalak, S. E.; Wiley, B. J.; Kim, M.; Formo, E. V.; Xia, Y. On the Polyol Synthesis of Silver Nanostructures: Glycolaldehyde as a Reducing Agent. *Nano Lett.* **2008**, *8*, 2077−2081.

(38) Velev, O. D.; Gupta, S. Materials Fabricated by Micro and Nanoparticle Assembly − The Challenging Path from Science to Engineering. *Adv. Mater.* **2009**, *21*, 1897−1905.

(39) Jiang, P.; Bertone, J. F.; Hwang, K. S.; Colvin, V. Single-Crystal Colloidal Multilayers of Controlled Thickness. *Chem. Mater.* **1999**, *11*, 2132−2140.

(40) Wong, S.; Kitaev, V.; Ozin, G. O. Colloidal Crystal Films: Advances in Universality and Perfection. *J. Am. Chem. Soc.* **2003**, *125*, 15589−15598.

(41) Masuda, Y.; Itoh, Y.; Koumoto, K. Self-Assembly Patterning of Silica Colloidal Crystals. *Langmuir* **2005**, *21*, 4478−4481.